Four-level model of ion–ion laser-induced collisional energy transfer and numerical calculations for Ca^+–Sr^+ system*

Chen De-Ying(陈德应)†, Zhang Hong-Ying(张洪英), and Fan Rong-Wei(樊荣伟)

National Key Laboratory of Tunable Laser Technology, Institute of Opto-Electronics, Harbin Institute of Technology, Harbin 150001, *China*

(Received 14 April 2009; revised manuscript received 21 August 2009)

The four-level model of laser-induced collisional energy transfer (LICET) for the ion–ion collision system is established based on the time-dependent Schrödinger equation for the electron dynamics, through which the equations of motion of the probability amplitudes and cross section of the collision system are obtained. Numerical calculations are performed for the Ca^+–Sr^+ system, with the results showing that the peak of the LICET spectrum appears at a resonant frequency of the transfer laser. The magnitude of the obtained collision cross section is in the order of 10^{-16} cm^2, and is comparable to that obtained in atomic systems, which indicates the validity of the established four-level model.

Keywords: laser-induced collisional energy transfer, four-level model, Ca^+–Sr^+ system
PACC: 3450R, 3490

1. Introduction

It is known that the cross section of an inelastic collision between two different particles (atoms or ions) is infinitesimally small if the energy defect ΔE between the initial and the final states of the two particles is large with respect to kT (typically the cross section is smaller than 10^{-20} cm^2). Large cross sections of interparticle collisions can be obtained by applying a laser field with a frequency at $\hbar\Omega = \Delta E$. The inelastic collision process of this type, which is known as laser-induced collisional energy transfer (LICET), was first predicted by Gudzenkoand Yakovlenko.[1] In the presence of a laser field (the transfer laser) with a properly selected frequency which can introduce or 'switch' the collision process, the cross sections of interparticle collision will be significantly increased to even above 10^{-13} cm^2,[2] allowing fast and efficient energy transfer between non-resonant states of the two colliding particles.

The first experimental observation of the LICET process is believed to be the collision process in the Sr–Ca system reported by Harris and co-operators[3] in 1977. To date, the LICET processes in several atomic systems such as Eu–Sr,[4−7] Sr–Ca,[8] Rb–K,[9] Rb–Na[10] and Li–Sr,[11] as well as the charge transfer,[12] charge exchange[13] and collisional ionization,[14] have been demonstrated, both theoretically and experimentally. In recent years, the issues of laser-induced or assisted collisions have attracted considerable interests[15−18] because of their potential abilities to control both the relative and absolute probabilities of competing exit channels by adjusting laser parameters such as wavelength, intensity, etc. However, for many years studies have been limited to atom–atom and atom–ion systems. To the best of our knowledge, neither theoretical nor experimental studies on LICET in ion–ion systems have been reported up to now. Ions involved collisions exploit a high-capacity storage species, i.e. ground-state ions which can be easily created and have long lifetimes, and are of particular interest because of their relevance to laser and plasma physics[19] and the inherent high detection sensitivity of charged particles, especially for gaseous ions that can be easily detected through time-of-flight (TOF) mass spectrometry.[20]

In this paper, the LICET process between two ions is looked upon as a four-body system, for which the time-dependent Schrödinger equation is offered. Based on the semiclassical approximation assuming straight-line trajectories of the ions, the equations of motion for the probability amplitudes of the system

*Project supported by the National Natural Science Foundation of China (Grant Nos. 10674036 and 10774033) and Program of Excellent Team in Harbin Institute of Technology, China.
†Corresponding author. E-mail: dychen@hit.edu.cn
© 2010 Chinese Physical Society and IOP Publishing Ltd

are obtained. As an application of this theoretical model, the LICET process in Ca^+–Sr^+ system is numerically calculated, which is anticipated to provide a theoretical reference for potential experimental studies on LICET between two ions.

2. The theoretical model

LICET between two ions can be described by the following expression:

$$A^{+*} + B^+ + \hbar\Omega \rightarrow A^+ + B^{+**}, \tag{1}$$

or by Fig. 1, in which only the energy levels of ions A^+ and B^+ relevant to the LICET process are present. LICET occurs between states $|A^{+*}\rangle$ and $|B^{+**}\rangle$. The asterisks indicate that excited states of pertinent ions are involved.

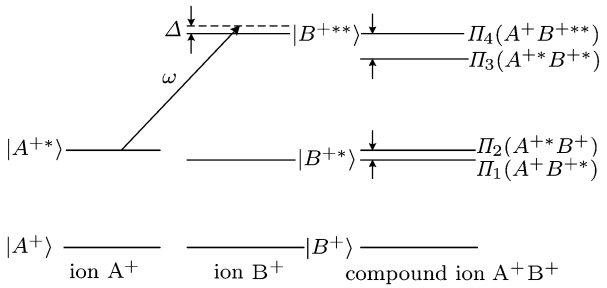


Fig. 1. Energy levels of LICET between two ions.

In order to obtain the equation of motion for the probability amplitudes of the LICET in an ion–ion system, the following assumptions are necessary:

(i) The ions follow the classical motion law and move with uniform velocities during the LICET process,

(ii) The laser field is regarded as a classical electric field, whose intensity remains unchanged during the collision,

(iii) The mass motion of the ions in the laser field can be described by a mean potential which remains unchanged during the whole collision process,

(iv) Only two colliding ions are involved in the collisional energy transfer process at one time.

2.1. The time-dependent Schrödinger equation

We start with the time-dependent Schrödinger equation for the whole system

$$\mathrm{i}\hbar\frac{\partial\varphi}{\partial t} = E\varphi = (T+V)\varphi, \tag{2}$$

where E is the total energy of the whole system, T and V are the kinetic energy and potential energy operators, respectively.

LICET between ions A^+ and B^+ can be described by a four-body system shown in Fig. 2, where e_1 and e_2 denote bound electrons of ions A^+ and B^+, respectively.

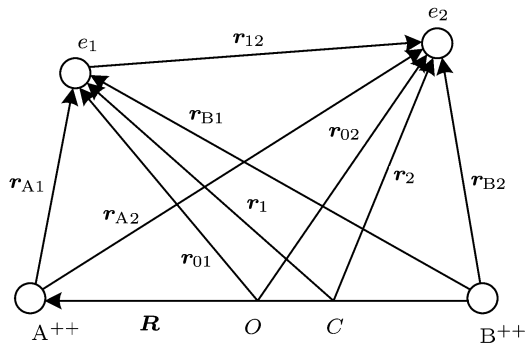


Fig. 2. Scheme of the four-body system of LICET between two ions.

In Fig. 2, $\boldsymbol{R}$ is the position vector between the two ion cores. $\boldsymbol{r}_{A1}$, $\boldsymbol{r}_{A2}$, $\boldsymbol{r}_{B1}$ and $\boldsymbol{r}_{B2}$ are the position vectors of electrons e_1 and e_2 with respect to their ion cores, respectively; $\boldsymbol{r}_1$ and $\boldsymbol{r}_2$ are the position vectors of electrons e_1 and e_2 with respect to the centroid C, respectively; $\boldsymbol{r}_{01}$ and $\boldsymbol{r}_{02}$ are the position vectors of electrons e_1 and e_2 with respect to the centre of the two ion cores O, respectively. Therefore, the kinetic energy and potential energy operators of the four-body system in the centre of mass coordinate system (i.e. $\boldsymbol{R}$, $\boldsymbol{r}_1$ and $\boldsymbol{r}_2$) can be expressed as

$$T = -\frac{\hbar^2}{2\mu_\mathrm{e}}\nabla_{r_1}^2 - \frac{\hbar^2}{2\mu_\mathrm{e}}\nabla_{r_2}^2 - \frac{\hbar^2}{2\mu_\mathrm{n}}\nabla_R^2, \tag{3}$$

$$V = V_{\mathrm{A^{++}B^{++}}} + V_{\mathrm{A^{++}e1}} + V_{\mathrm{A^{++}e2}} + V_{\mathrm{B^{++}e1}} + V_{\mathrm{B^{++}e2}} + V_{\mathrm{e1e2}} + V_\mathrm{f}, \tag{4}$$

where μ_e and μ_n are the reduced masses of the two electrons and the two ion cores, respectively. V_f is the interaction between the laser field and the colliding particles.

The motion of the two ion cores can be described by wave function $F(\boldsymbol{R})$ which meets the following scattering equation

$$\left[-\frac{\hbar^2}{2\mu_\mathrm{n}}\nabla_R^2 - E\right]F(\boldsymbol{R}) = 0. \tag{5}$$

Then the total wave function of the system, i.e. $\varphi(\boldsymbol{R},\ \boldsymbol{r}_1,\ \boldsymbol{r}_2)$, can be written as the product of $F(\boldsymbol{R})$ and the wave function of the electrons $\psi(\boldsymbol{R},\ \boldsymbol{r}_1,\ \boldsymbol{r}_2)$

$$\varphi(\boldsymbol{R},\ \boldsymbol{r}_1,\ \boldsymbol{r}_2) = F(\boldsymbol{R})\psi(\boldsymbol{R},\ \boldsymbol{r}_1,\ \boldsymbol{r}_2). \tag{6}$$

Substituting the Eq. (6) into the Schrödinger equation (2), we can obtain

$$\begin{aligned} &-\frac{\hbar^2}{2\mu_{\rm n}}F(\boldsymbol{R})\nabla_R^2\psi(\boldsymbol{R},\ \boldsymbol{r}_1,\ \boldsymbol{r}_2)\\ &-\frac{\hbar^2}{\mu_{\rm n}}\nabla_R F(\boldsymbol{R})\cdot\nabla_R\psi(\boldsymbol{R},\ \boldsymbol{r}_1,\ \boldsymbol{r}_2)\\ &+F(\boldsymbol{R})H_{\rm e}\psi(\boldsymbol{R},\ \boldsymbol{r}_1,\ \boldsymbol{r}_2)=0, \end{aligned} \tag{7}$$

where

$$H_{\rm e}=-\frac{\hbar^2}{2\mu_{\rm e}}\nabla_{r_1}^2-\frac{\hbar^2}{2\mu_{\rm e}}\nabla_{r_2}^2+V. \tag{8}$$

The first two terms in Eq. (7) describe the coupling of motions of the ion cores and the electrons.

For a classical straight-line trajectory (discussed in detail in Section 2.2) in which the relative velocity is parallel to the z axis, $F(\boldsymbol{R})$ is a plane wave in the form

$$F(\boldsymbol{R})=\exp\left(\mathrm{i}\,\frac{\mu}{\hbar}\cdot z_R\right), \tag{9}$$

where $z_R=vt$.

Substituting Eq. (9) into Eq. (7), the first term can be omitted because the reduced mass $\mu_{\rm n}$ is a large parameter; Equation (7) can be rewritten as

$$H_{\rm e}\psi(\boldsymbol{R},\ \boldsymbol{r}_1,\ \boldsymbol{r}_2)=\mathrm{i}\,\hbar v\frac{\partial}{\partial z_R}\psi(\boldsymbol{R},\ \boldsymbol{r}_1,\ \boldsymbol{r}_2). \tag{10}$$

Then Eq. (10) can be rewritten as a time-dependent Schrödinger equation as follows:

$$H_{\rm e}\psi(\boldsymbol{r}_1,\ \boldsymbol{r}_2,\ t)=\mathrm{i}\,\hbar\frac{\partial}{\partial t}\psi(\boldsymbol{r}_1,\ \boldsymbol{r}_2,\ t), \tag{11}$$

where $\psi(\boldsymbol{r}_1,\ \boldsymbol{r}_2,\ t)$ is the wave function of the electrons.

2.2. The equations of motion

We consider a classical straight-line path shown in Fig. 3, which is similar to that described in Ref. [8], where ion B^+ is fixed and ion A^+ moves in a straight line with a velocity v along the z-axis. The relative distance of the two ions, as a function of time, is $R^2(t)=b^2+v^2t^2$, where b is termed the impact parameter.

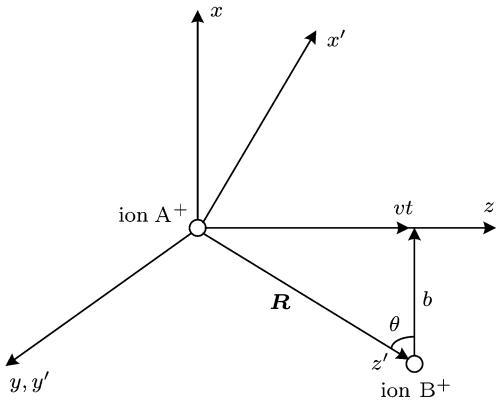


Fig. 3. Coordinate system of the straight-line path.

The unprimed system is fixed in space, while in the primed system, the z'-axis points along the interatomic axis, and therefore rotates with respect to the unprimed system during the collision, i.e.

$$x=x'\sin\theta-z'\cos\theta, \tag{12}$$

$$y=y', \tag{13}$$

$$z=x'\cos\theta+z'\sin\theta, \tag{14}$$

where $\cos\theta=b/R(t)$. During the course of the collision θ varies from $-\pi/2$ to $\pi/2$.

We assume that the incident laser beam has frequency ω and is polarised along the y-axis, i.e. $\boldsymbol{E}(t)=\boldsymbol{a}_y\varepsilon\cos(\omega t)$. Then the classical interaction Hamiltonian may be written as

$$\begin{aligned} H(t)=&\frac{e^2}{4\pi\varepsilon_0R^3}(x'_{\rm A1}x'_{\rm B2}+y'_{\rm A1}y'_{\rm B2}-2z'_{\rm A1}z'_{\rm B2})\\ &+\frac{3e^2}{4\pi\varepsilon_0R}-\frac{e^2}{4\pi\varepsilon_0r_{\rm A2}}\\ &-\frac{e^2}{4\pi\varepsilon_0r_{\rm B1}}-e(y'_{\rm A1}+y'_{\rm B2})\varepsilon\cos(\omega t). \end{aligned} \tag{15}$$

The coordinates $x_{\rm A}$, $x_{\rm B}$, $x'_{\rm A}$, $x'_{\rm B}$ etc. denote the position of each electron with respect to its ion core.

For the four-level system of laser-induced collisional energy transfer between two ions A^+ and B^+ shown in Fig. 1, the following four levels of the A^+B^+ compound system can be formed by the energy levels of ion A^+ and B^+ as follows:

$$\Pi_1(\boldsymbol{r}_1,\ \boldsymbol{r}_2,\ t)=\chi_1(\boldsymbol{r}_{\rm A1})\varphi_2(\boldsymbol{r}_{\rm B2})\cdot\exp[\mathrm{i}(\alpha_1+\beta_2)], \tag{16}$$

$$\Pi_2(\boldsymbol{r}_1,\ \boldsymbol{r}_2,\ t)=\chi_2(\boldsymbol{r}_{\rm A1})\varphi_1(\boldsymbol{r}_{\rm B2})\cdot\exp[\mathrm{i}(\alpha_2+\beta_1)], \tag{17}$$

$$\Pi_3(\boldsymbol{r}_1,\ \boldsymbol{r}_2,\ t)=\chi_2(\boldsymbol{r}_{\rm A1})\varphi_2(\boldsymbol{r}_{\rm B2})\cdot\exp[\mathrm{i}(\alpha_2+\beta_2)], \tag{18}$$

$$\Pi_4(\boldsymbol{r}_1,\ \boldsymbol{r}_2,\ t)=\chi_1(\boldsymbol{r}_{\rm A1})\varphi_3(\boldsymbol{r}_{\rm B2})\cdot\exp[\mathrm{i}(\alpha_1+\beta_3)], \tag{19}$$

where α_i and β_j take the following forms:

$$\alpha_i = -\frac{\eta_i}{\hbar}t + \frac{\mu_e}{\hbar}p\boldsymbol{v}\cdot\boldsymbol{r}_1 - \frac{\mu_e}{2\hbar}p^2\boldsymbol{v}^2t, \tag{20}$$

$$\beta_j = -\frac{\varepsilon_j}{\hbar}t - \frac{\mu_e}{\hbar}q\boldsymbol{v}\cdot\boldsymbol{r}_2 - \frac{\mu_e}{2\hbar}q^2\boldsymbol{v}^2t, \tag{21}$$

with η_i and ε_j being eigenvalues of $\chi_1(\boldsymbol{r}_{A1})$ and $\varphi_2(\boldsymbol{r}_{B2})$, respectively; p and q in formulae (20) and (21) are defined by

$$p = \frac{M_B}{M_A + M_B}, \tag{22}$$

$$q = \frac{M_A}{M_A + M_B}, \tag{23}$$

where M_A and M_B are the masses of ions A and B, respectively.

Expanding the wave function of the electrons using the primary functions $\psi(\boldsymbol{R},\ \boldsymbol{r}_1,\ \boldsymbol{r}_2)$ expressed by formulae (16)–(19),

$$\psi(\boldsymbol{r}_1,\ \boldsymbol{r}_2,\ t) = \sum_i c_i \Pi_i(\boldsymbol{r}_1,\ \boldsymbol{r}_2,\ t). \tag{24}$$

Then the equations of motion for the probability amplitudes can be obtained as

$$\mathrm{i}\,\hbar\dot{\boldsymbol{C}} = \boldsymbol{H}\boldsymbol{C}, \tag{25}$$

where

$$\boldsymbol{C} = \begin{bmatrix} c_1 \\ c_2 \\ c_3 \\ c_4 \end{bmatrix} \tag{26}$$

and H is a 4×4 matrix with its elements defined by

$$H_{ij} = \int \mathrm{d}^3r_1 \int \mathrm{d}^3r_2 \Pi_i(r_1,\ r_2,\ t)H(t) \times \Pi_j(r_1,\ r_2,\ t). \tag{27}$$

2.3. Collision cross section

Taking the following unitary transformation of matrix $\boldsymbol{C}$:

$$\boldsymbol{a}(t) = \boldsymbol{T}(t)\cdot\boldsymbol{C}(t), \tag{28}$$

where

$$\boldsymbol{T}(t) = \begin{bmatrix} \exp(-\mathrm{i}\,\omega_{12}t) & 0 & 0 & 0 \\ 0 & 1 & 0 & 0 \\ 0 & 0 & \exp[-\mathrm{i}(\omega_{32}-\Omega)t] & 0 \\ 0 & 0 & 0 & \exp[-\mathrm{i}(\omega_{42}-\Omega)t] \end{bmatrix}, \tag{29}$$

$$\omega_{mn} = (E_m - E_n)/\hbar, \tag{30}$$

the equation of motion for the probability amplitudes can be obtained as:

$$\mathrm{i}\,\dot{\boldsymbol{a}} = \boldsymbol{V}\boldsymbol{a}, \tag{31}$$

where

$$\boldsymbol{a} = \begin{bmatrix} a_1 \\ a_2 \\ a_3 \\ a_4 \end{bmatrix}, \tag{32}$$

and

$$\boldsymbol{V} = \begin{bmatrix} -\omega_{21} + V_{11} & V_{12} & V_{13} & V_{14} \\ V_{21} & V_{22} & V_{23} & 0 \\ V_{31} & V_{32} & \omega_{32} - \omega + V_{33} & V_{34} \\ V_{41} & 0 & V_{43} & \omega_{43} - \omega + V_{44} \end{bmatrix}. \tag{33}$$

The E_n in Eq. (30) are the sum energies of the pertinent states of the infinitely separated ions described by Π_n in Eqs. (16)–(19), and are not functions of position or time. Equation (31) meets the initial conditions that

$$\begin{cases} |a_1(-\infty)|^2 = 0, \\ |a_2(-\infty)|^2 = 1, \\ |a_3(-\infty)|^2 = 0, \\ |a_4(-\infty)|^2 = 0. \end{cases} \tag{34}$$

Using the interaction Hamiltonian $H(t)$ in formula (15) and the primary functions expressed by formulae (16)–(19), we can derive the elements of matrix $\boldsymbol{V}$

$$V_{11} = \frac{e^2}{4\pi\varepsilon_0\hbar}\left[\frac{3}{R} - \int \mathrm{d}^3 r_{\mathrm{B}2}\frac{1}{r_{\mathrm{A}2}}|\varphi_2(\boldsymbol{r}_{\mathrm{B}2})|^2 - \int \mathrm{d}^3 r_{\mathrm{A}1}\frac{1}{r_{\mathrm{B}1}}|\chi_1(\boldsymbol{r}_{\mathrm{A}1})|^2\right], \tag{35}$$

$$V_{12} = \frac{e^2}{4\pi\varepsilon_0\hbar R^3}\int \mathrm{d}^3 r_{\mathrm{A}1}\int \mathrm{d}^3 r_{\mathrm{B}2}\,(x'_{\mathrm{A}1}x'_{\mathrm{B}2} + y'_{\mathrm{A}1}y'_{\mathrm{B}2} - 2z'_{\mathrm{A}1}z'_{\mathrm{B}2}) \times \chi_1^*(\boldsymbol{r}_{\mathrm{A}1})\varphi_2^*(\boldsymbol{r}_{\mathrm{B}2})\chi_2(\boldsymbol{r}_{\mathrm{A}1})\varphi_1(\boldsymbol{r}_{\mathrm{B}2}), \tag{36}$$

$$V_{13} = -\frac{1}{2\hbar}e\varepsilon\int \mathrm{d}^3 r_{\mathrm{A}1}y'_{\mathrm{A}1}\chi_1^*(\boldsymbol{r}_{\mathrm{A}1})\chi_2(\boldsymbol{r}_{\mathrm{A}1}), \tag{37}$$

$$V_{14} = -\frac{1}{2\hbar}e\varepsilon\int \mathrm{d}^3 r_{\mathrm{B}2}y'_{\mathrm{B}2}\varphi_2^*(\boldsymbol{r}_{\mathrm{B}2})\varphi_3(\boldsymbol{r}_{\mathrm{B}2}), \tag{38}$$

$$V_{22} = \frac{e^2}{4\pi\varepsilon_0\hbar}\left[\frac{3}{R} - \int \mathrm{d}^3 r_{\mathrm{B}2}\frac{1}{r_{\mathrm{A}2}}|\varphi_1(\boldsymbol{r}_{\mathrm{B}2})|^2 - \int \mathrm{d}^3 r_{\mathrm{A}1}\frac{1}{r_{\mathrm{B}1}}|\chi_2(\boldsymbol{r}_{\mathrm{A}1})|^2\right], \tag{39}$$

$$V_{23} = -\frac{1}{2\hbar}e\varepsilon\int \mathrm{d}^3 r_{\mathrm{B}2}y'_{\mathrm{B}2}\varphi_1^*(\boldsymbol{r}_{\mathrm{B}2})\varphi_2(\boldsymbol{r}_{\mathrm{B}2}), \tag{40}$$

$$V_{24} = 0, \tag{41}$$

$$V_{33} = \frac{e^2}{4\pi\varepsilon_0\hbar}\left[\frac{3}{R} - \int \mathrm{d}^3 r_{\mathrm{B}2}\frac{1}{r_{\mathrm{A}2}}|\varphi_2(\boldsymbol{r}_{\mathrm{B}2})|^2 - \int \mathrm{d}^3 r_{\mathrm{A}1}\frac{1}{r_{\mathrm{B}1}}|\chi_2(\boldsymbol{r}_{\mathrm{A}1})|^2\right], \tag{42}$$

$$V_{34} = \frac{e^2}{4\pi\varepsilon_0\hbar R^3}\int \mathrm{d}^3 r_{\mathrm{A}1}\int \mathrm{d}^3 r_{\mathrm{B}2}\,(x'_{\mathrm{A}1}x'_{\mathrm{B}2} + y'_{\mathrm{A}1}y'_{\mathrm{B}2} - 2z'_{\mathrm{A}1}z'_{\mathrm{B}2}) \times \chi_2^*(\boldsymbol{r}_{\mathrm{A}1})\varphi_2^*(\boldsymbol{r}_{\mathrm{B}2})\chi_1(\boldsymbol{r}_{\mathrm{A}1})\varphi_3(\boldsymbol{r}_{\mathrm{B}2}), \tag{43}$$

$$V_{44} = \frac{e^2}{4\pi\varepsilon_0\hbar}\left[\frac{3}{R} - \int \mathrm{d}^3 r_{\mathrm{B}2}\frac{1}{r_{\mathrm{A}2}}|\varphi_3(\boldsymbol{r}_{\mathrm{B}2})|^2 - \int \mathrm{d}^3 r_{\mathrm{A}1}\frac{1}{r_{\mathrm{B}1}}|\chi_1(\boldsymbol{r}_{\mathrm{A}1})|^2\right], \tag{44}$$

$$V_{mn} = V_{nm}^*. \tag{45}$$

Then the expression of the collision cross section can be obtained

$$\sigma = 2\pi\int_0^\infty |a_4(b, +\infty)|^2 b\cdot \mathrm{d}b. \tag{46}$$

3. Application to Ca^+–Sr^+ system

The LICET process in Ca^+–Sr^+ system, for which we perform the numerical calculations, can be expressed as

$$\mathrm{Ca}^+(4\mathrm{p}\ ^2P_{3/2}) + \mathrm{Sr}^+(5\mathrm{s}\ ^2S_{1/2}) + \hbar\Omega(448\ \mathrm{nm}) \rightarrow \mathrm{Ca}^+(4\mathrm{s}\ ^2S_{1/2}) + \mathrm{Sr}^+(6\mathrm{s}\ ^2S_{1/2}) \tag{47}$$

with the corresponding energy level scheme shown in Fig. 4. Before laser-induced collision takes place, Ca^+ is initially prepared in its excited state $Ca^+(4p\ ^2P_{3/2})$, and Sr^+ is in its ground state $Sr^+(5s\ ^2S_{1/2})$.

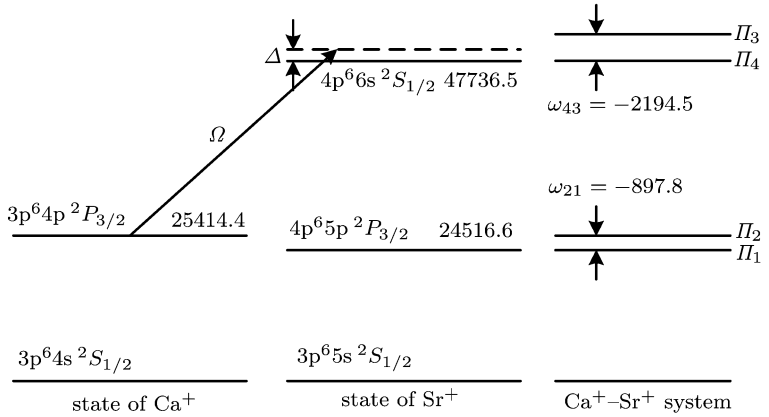


Fig. 4. Energy levels of LICET in Ca^+–Sr^+ system. LICET occurs between states $Ca^+(3p^6 4p\ ^2P_{3/2})$ and $Sr^+(4p^6 6s\ ^2S_{1/2})$. The energy levels are given in cm^{-1}.

With the transfer laser tuned resonant with the interparticle transition present, laser-induced collision between Ca^+ and Sr^+ takes place, with the result that Ca^+ returns to its ground state $Ca^+(4s\ ^2S_{1/2})$ due to collision deexcitation, while Sr^+ transfers to a higher excited state $Sr^+(6s\ ^2S_{1/2})$ with simultaneous absorption of a laser photon and the excitation energy of Ca^+. The Δ denotes the laser detuning from the resonant transition frequency, i.e. $\Delta = \omega - \omega_{42}$. As shown in Fig. 4, the intermediate energy level $Sr^+(5p\ ^2P_{3/2})$ is also involved in LICET.

For the Ca^+–Sr^+ system shown in Fig. 4, the four energy levels of the combined system can be expressed as

$$\left.\begin{aligned}
\Pi_1(\boldsymbol{r}_1,\boldsymbol{r}_2,t) &= \chi_{Ca^+(4s)}(\boldsymbol{r}_{A1})\varphi_{Sr^+(5p)}(\boldsymbol{r}_{B2})\cdot\exp[\mathrm{i}(\alpha_1+\beta_2)]\\
\Pi_2(\boldsymbol{r}_1,\boldsymbol{r}_2,t) &= \chi_{Ca^+(4p)}(\boldsymbol{r}_{A1})\varphi_{Sr^+(5s)}(\boldsymbol{r}_{B2})\cdot\exp[\mathrm{i}(\alpha_2+\beta_1)]\\
\Pi_3(\boldsymbol{r}_1,\boldsymbol{r}_2,t) &= \chi_{Ca^+(4p)}(\boldsymbol{r}_{A1})\varphi_{Sr^+(5p)}(\boldsymbol{r}_{B2})\cdot\exp[\mathrm{i}(\alpha_2+\beta_2)]\\
\Pi_4(\boldsymbol{r}_1,\boldsymbol{r}_2,t) &= \chi_{Ca^+(4s)}(\boldsymbol{r}_{A1})\varphi_{Sr^+(6s)}(\boldsymbol{r}_{B2})\cdot\exp[\mathrm{i}(\alpha_1+\beta_3)]
\end{aligned}\right\} \tag{48}$$

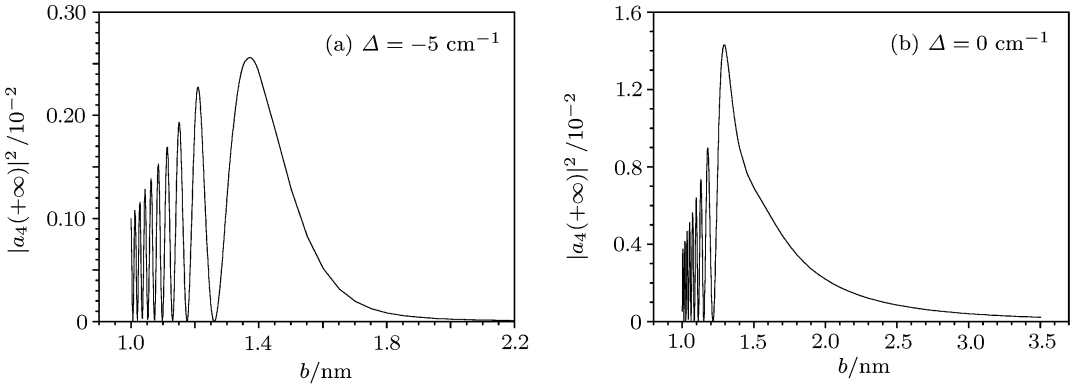
with α_i and β_j defined in formulae (20) and (21) respectively.

In Eq. (48) $\boldsymbol{r}_{A1}$ and $\boldsymbol{r}_{B2}$ are the position vectors of the bound electrons in ions Ca^+ and Sr^+ with respect to their respective ion core; $\boldsymbol{r}_1$ and $\boldsymbol{r}_2$ are the position vectors of the bound electrons with respect to the centroid of the whole system; η_1 and η_2 are energy eigenvalues of states $(4s\ ^2S_{1/2})$ and $(4p\ ^2P_{3/2})$ of Ca^+, respectively; ε_1, ε_2, and ε_3 are energy eigenvalues of states $(5s\ ^2S_{1/2})$, $(5p\ ^2P_{3/2})$, and $(6s\ ^2S_{1/2})$ of Sr^+, respectively.

When the transfer laser is tuned nearly resonant with the transition $Ca^+(4p\ ^2P_{3/2}) \rightarrow Sr^+(6s\ ^2S_{1/2})$, assuming that the electric-field intensity of the transfer laser is 10^7 V/m (the corresponding power density is 1.33×10^7 W/cm^2), the theoretical values of the elements of matrix $\boldsymbol{V}$ are

$$\boldsymbol{V} = \begin{bmatrix}
-\omega_{21}+V_{11} & \dfrac{3.929\times10^{-14}}{R^3} & -1.373\times10^{12}\,\mathrm{i} & -9.972\times10^{11}\,\mathrm{i}\\
\dfrac{3.929\times10^{-14}}{R^3} & V_{22} & -1.506\times10^{12}\,\mathrm{i} & 0\\
1.373\times10^{12}\,\mathrm{i} & 1.506\times10^{12}\,\mathrm{i} & \omega_{32}-\Omega+V_{33} & \dfrac{7.780\times10^{-14}}{R^3}\\
9.972\times10^{11}\,\mathrm{i} & 0 & \dfrac{7.780\times10^{-14}}{R^3} & \omega_{42}-\Omega+V_{44}
\end{bmatrix}. \tag{49}$$

Based on the theoretically calculated matrix $\boldsymbol{V}$ expressed by formula (49), the transition probability $|a_4(+\infty)|^2$ as a function of the impact parameter b for this Ca^+–Sr^+ system is numerically calculated. When the relative velocity between the two colliding ions is 600 m/s, and the laser detunings are -5, 0, 5 and 10 cm^{-1} respectively, the results of calculation are shown in Fig. 5. It can be seen from Fig. 5 that the transition probability reaches a maximum in the vicinity of the relative Weisskopf radius b_0,[8] and the transition probability oscillates with decreasing b for impact parameters less than b_0.



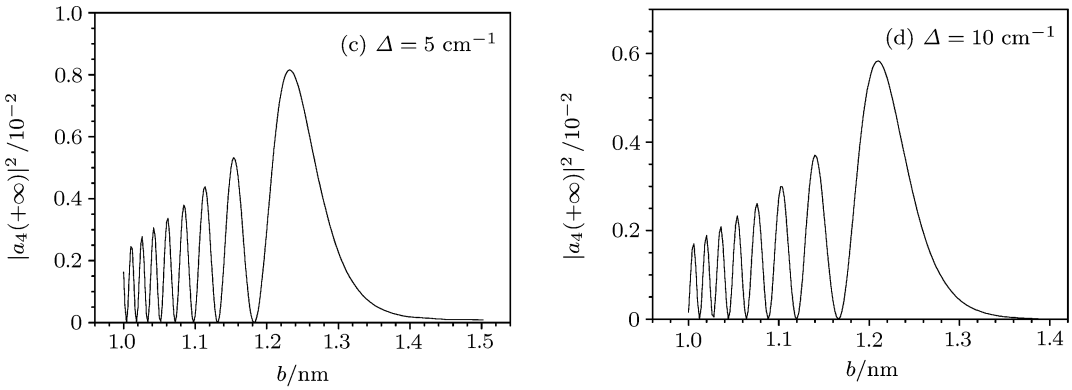


Fig. 5. The transition probability versus the impact parameter for the Ca^+–Sr^+ system.

To reduce the computational complexity, first of all it is necessary to determine the integrating range of the impact parameter b when calculating the cross section of LICET in Ca^+–Sr^+ system. For the integrand in formula (46), which is the product of the transition probability $|a_4(+\infty)|^2$ and the impact parameter b, on one hand, contribution of collisional transition to the cross section is proportional to the impact parameter b; on the other hand, from Fig. 5 one can see that the transition probability $|a_4(+\infty)|^2$ obviously has a cut-off value where the impact parameter b is relatively large, and it asymptotically becomes zero when b goes on increasing, in which case its contribution to the cross section can be neglected. As to the collision cross section for this Ca^+–Sr^+ system, the calculation precision can be sufficiently ensured with the integrating range of b set at [1 nm, 5 nm].

The cross section of LICET in the Ca^+–Sr^+ system versus laser detuning Δ (i.e. the LICET spectrum), calculated with the laser field intensity fixed at 10^7 W/cm^2, is shown in Fig. 6, where the four curves from the top to the bottom are the results when the relative velocity between the two colliding ions is fixed at 500, 600, 700, and 800 m/s, respectively, and their corresponding full width at half maximum (FWHM, i.e. tuning range) is 2.6, 3.1, 3.6, and 4.1 cm^{-1}, respectively. From Fig. 6 one can see that the LICET line shape is nearly symmetrical at the centre, which is similar to the case in atomic systems.[11] The calculated magnitude of the collision cross section, which is in the order of 10^{-16} cm^2, is comparable to that experimentally obtained in the Ca^+–Sr system under similar conditions. It can be seen from Fig. 6 that the peak of the LICET profile appears at a laser detuning of $\Delta = 0$ cm^{-1}, which is consistent with the theoretical analysis. Moreover, with the same field intensity of the transfer laser, cross section of LICET in the Ca^+–Sr^+ system shows a tendency of decline, while the tuning range of the cross section increases as the relative velocity increases. However, the relative velocity between the two colliding ions has no impact on the position of the line peak.

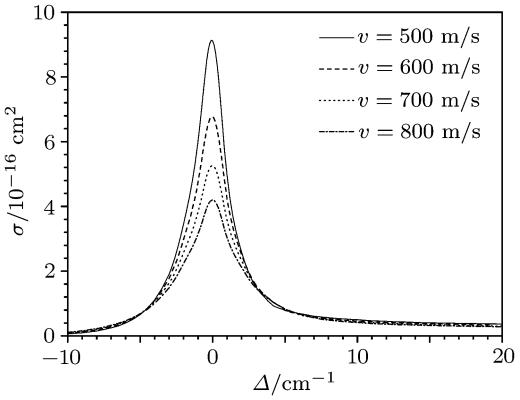


Fig. 6. The collision cross section versus laser detuning for the Ca^+–Sr^+ system.

4. Conclusion

Based on the semiclassical approximation assuming straight-line trajectories of the ions and a four state expansion of the time-dependent Schrödinger equation for the electron dynamics, we develop a four-level theoretical model for the ion–ion LICET system. As an example of its application, a LICET process in the Ca^+–Sr^+ system is numerically calculated, and the LICET profiles at different relative velocities are obtained. The numerical results show that the peak of the LICET spectrum appears when the transfer laser is tuned resonant with the interparticle transi-

tion. The magnitude of the obtained collision cross section which is in the order of 10^{-16} cm^2, is anticipated to provide a theoretical reference for potential experimental studies on LICET between two ions. We hope that the four-level model developed in this paper will apply to other ion–ion systems; however, more examinations are still needed to further prove the validity of the model. Potential experimental studies are expected on ionic metal mixtures in the heat-pipe oven traditionally used for experiments of atom–atom and ion–atom systems, or on gaseous ion systems for which TOF mass spectrometry can be used.

References

[1] Gudzenko L I and Yakovlenko S I 1972 *Sov. Phys.-JETP* **35** 877

[2] Green W R, Lukasik J, Willison J R, Wright M D, Young J F and Harris S E 1979 *Phys. Rev. Lett.* **42** 970

[3] Falcone R W, Green W R, White J C, Young J F and Harris S E 1977 *Phys. Rev.* A **15** 1333

[4] Mazzoni M and Fini L 1993 *Phys. Rev.* A **48** 3786

[5] Bambini A and Geltman S 1994 *Phys. Rev.* A **50** 5081

[6] Buffa R, Cavalieri S, Eramo R and Fini L 1995 *Phys. Rev.* A **52** 1382

[7] Zhang H Y, Xia Y Q, Chen D Y, Xiao P, Fan R W and Ma Z G 2005 *Sci. in China* Ser. G **48** 78

[8] Harris S and White J 1977 *IEEE J. Quantum Electron.* **13** 972

[9] Cheron B and Mosaddak S 1985 *Opt. Commun.* **54** 7

[10] Cheron B, Kucal H and Hennecart D 1990 *J. Phys.* B: *At. Mol. Opt. Phys.* **23** 4281

[11] Geltman S 1992 *Phys. Rev.* A **45** 4792

[12] Geltman S 1987 *Phys. Rev.* A **35** 3775

[13] Débarre A and Cahuzac P 1986 *J. Phys.* B: *At. Mol. Phys.* **19** 3965

[14] Buffa R 1995 *Opt. Lett.* **20** 204

[15] Simeoni R J, Peach G and Whittingham I B 1997 *J. Phys.* B: *At. Mol. Opt. Phys.* **30** 1071

[16] Lein M and Rost J M 2003 *Phys. Rev. Lett.* **91** 243901

[17] Anis F, Roudnev V, Cabrera-Trujillo R and Esry B D 2006 *Phys. Rev.* A **73** 043414

[18] Zhang H Y, Lu Z Z, Fan R W and Chen D Y 2008 *Chin. Phys.* B **17** 4504

[19] Jiao R Z and Feng C X 2008 *Chin. Phys.* B **17** 1845

[20] Guilhaus M, Mlynski V and Selby D 1997 *Rapid Commun. Mass Spectrom.* **11** 951